Laser-induced Autofluorescence Spectral Ratio Reference Standard for Early Discrimination of Oral Cancer

Rupananda J. Mallia, MSc[1]
Shiny Sara Thomas, MSc[1]
Anitha Mathews, MD[2]
Rejnish Kumar R, MD[3]
Paul Sebastian, MS[4]
Jayaprakash Madhavan, MD[5]
Narayanan Subhash, PhD[1]

[1] Biophotonics Laboratory, Center for Earth Science Studies, Trivandrum, India.

[2] Department of Cytopathology, Regional Cancer Center, Trivandrum, India.

[3] Department of Radiation Oncology, Regional Cancer Center, Trivandrum, India.

[4] Division of Surgical Oncology, Regional Cancer Center, Trivandrum, India.

[5] Department of Radiotherapy, Regional Cancer Center, Trivandrum, India.

Supported by grants from the Department of Science & Technology (DST), Govt. of India, and the CESS Plan-223 project.

The authors thank the Research Council (RC) of the Center for Earth Science Studies (CESS) and the Institutional Review Board (IRB), Regional Cancer Center (RCC) for encouragement and support. R.J.M. acknowledges the DST and CSIR, New Delhi; S.S.T. acknowledges the RC for research fellowships. We thank all the healthy volunteers and patients who participated in the clinical trials and the postgraduate students who were associated in this study.

The Institutional Review Board (IRB) and the Ethics Committee (EC) of Regional Cancer Center (RCC), Trivandrum, approved the study of human beings as experimental subjects. All patients and volunteers before enrollment signed the informed consent form that details the methodology, protocol, associated risks and benefits of participation in the trial.

Address for reprints: Subhash Narayanan, MSc, PhD, Centre for Earth Science Studies, Biophotonics Laboratory, Thuruvikkal P.O., Akkulam, Trivandrum, Kerala 695031 India; Fax: (011) 91-4712442280; E-mail: subhashn@cessind.org

Received June 18, 2007; accepted October 16, 2007.

BACKGROUND. Laser-induced autofluorescence (LIAF) is an emerging noninvasive technique in the biomedical field, especially for cancer detection. The goal of the study was to develop a spectral ratio reference standard (SRRS) to discriminate different grades of oral cancer.

METHODS. LIAF emission spectra from oral mucosa were recorded in the 420–720 nm spectral range on a miniature fiberoptic spectrometer from 14 anatomical sites of 35 healthy volunteers and 91 sites of 44 patients, with excitation at 404 nm from a diode laser.

RESULTS. Histopathologic analysis of biopsy samples showed that oral mucosa of adjoining malignant sites in patients are not usually normal, but showed various degrees of epithelial dysplasia and hyperplasia. Therefore, instead of using LIAF data from apparently normal lesions of patients as control, spectral data values of the oral mucosa of healthy volunteers were used as control. The autofluorescence emission at 500 nm is characteristic of oral mucosa, whereas in malignant lesions a new peak is seen at 685 nm in addition to the previously reported peaks at 635 and 705 nm. Three spectral ratio reference standard (SRRS) scatterplots were created to differentiate the normal mucosa from hyperplasia, hyperplasia from dysplasia, and dysplasia from squamous cell carcinoma (SCC) using the mean fluorescence intensity ratios (F500/F635, F500/705 and F500/F685) measured from 40 sites in 20 patients and 11 sites in 35 healthy volunteers. During blind tests at 21 sites in 17 patients all 3 SRRS plots showed 100% sensitivity and specificity to discriminate hyperplasia from dysplastic and normal tissues, whereas only the F500/F685 SRRS showed the same sensitivity and specificity to differentiate dysplasia from SCC.

CONCLUSIONS. An SRRS criteria based on scatterplots of autofluorescence spectral intensity ratios is described to discriminate oral mucosal variations and screen early stages of tissue progression toward malignancy. ***Cancer* 2008;112:1503–12.** © *2008 American Cancer Society.*

KEYWORDS: laser-induced autofluorescence spectroscopy, oral cavity squamous cell carcinoma, early detection of cancer, fluorescence intensity/ratios, spectral ratio reference standard.

Oral cavity cancer represents a significant health problem owing to its high rate of incidence, and oral carcinogenesis is a multistep process that usually arises in the superficial epithelial layer covering the lining of the body cavities. Eighty-five percent of oral

DOI 10.1002/cncr.23324
Published online 7 February 2008 in Wiley InterScience (www.interscience.wiley.com).

cavity malignancy is due to squamous cell carcinoma (SCC).[1] Oral epithelial dysplasias are precancerous lesions that appear clinically as erythroplakia and leukoplakia, with their chances of conversion to malignancy being approximately 90% and 10%, respectively.[2] The development of epithelial precancers is initiated through changes in nuclear shape, size, and density of cells and overall thickening of the epithelial layer.[3] Detection of neoplastic changes in the oral cavity relies heavily on visual examination by clinicians. Often, even for experienced clinicians, it is not easy to distinguish between normal and premalignant mucosa. Thus, biopsy of the site is the accepted clinical procedure for tissue diagnosis. A major hurdle here is to identify visually the most malignant location for biopsy and histopathologic diagnosis. As this is subjective, the chosen lesion may not always be appropriate and this often leads to repeated biopsies, to the discomfort of patients.

Despite tremendous advancements in ablative and reconstructive techniques for treating oral cancer, survival rates are not showing any significant improvement. These lower survival rates highlight the significance of developing adjunctive diagnostic tools that facilitate early detection of dysplastic changes in the oral cavity.

The prevalence of various optical spectroscopy techniques has been increasing and are getting greater recognition and acceptance these days owing to their noninvasive tissue characterization. The advantage of optical techniques over other methodologies is that they provide quantitative information that can be analyzed instantaneously and produce an objective diagnosis even in the hands of a less-skilled operator. Among these techniques the potential of laser-induced tissue autofluorescence is immense, but not fully explored for detection of precancerous lesions.

Many research groups have shown that techniques based on laser-induced autofluorescence (LIAF) spectroscopy is promising and fulfills the need for improved screening and diagnosis of cancer in the head and neck region and various other organs, like bronchus, colon, cervix, and esophagus.[4–9] Tissue fluorescence signatures are of significance because spectral changes reflect alterations in metabolic activity and communication between the epithelium and stroma. Autofluorescence arises because of emission from various fluorophores, such as elastin, collagen, and nicotinamide adenine dinucleotide (NADH) present in human tissue.[10,11] During the process of carcinogenesis, alterations occur in morphohistologic characteristics and physiochemical compositions of these cellular fluorophores, making LIAF spectral features sensitive to tissue alterations.

Various groups have carried out detailed studies of the autofluorescence spectra of oral mucosa and identified optimal excitation wavelengths for in vivo fluorescence detection of oral neoplasia.[12,13] On the basis of native tissue autofluorescence Gillenwater et al.[14] diagnosed oral cancer with 82% sensitivity and 100% specificity. Savage et al.[15] used different intensity ratios including red-blue ratios at various excitation wavelengths to differentiate malignant and normal lateral tongue.

Fluorescence imaging diagnostic systems were used by many researchers for instantaneous screening of the whole lesion area. Scott et al.[16] used a red-to-green fluorescence ratio imaging technique that showed good contrast enhancement between normal and cancerous lesions after topical application of 5-amino levulinic acid (5-ALA). Zheng et al.[17] developed a digitized endoscopic imaging system to classify normal, carcinoma in situ (CIS), and SCC of the oral cavity using red-to-blue fluorescence image ratios.

Svistun et al.[18] used a Canon SLR-camera with a 100-mm microlens and a broadband (60 nm) filter to photograph fluorescence emission from freshly resected oral lesions. They obtained a sensitivity of 91% and specificity of 86% for discrimination of normal tissue from neoplasia, which compared favorably with the white light sensitivity of 75% and specificity of 43%. That study also demonstrated that oral cavity fluorescence could be seen in real time by the naked eye. Very recently, Lane et al.[19] developed a simple, cost-effective, handheld device that allows clinicians to discriminate malignant tissue by direct visualization of tissue fluorescence. Clinical trials on 44 patients with this system gave a sensitivity of 98% and a specificity of 100% in discriminating normal mucosa from severe dysplasia.

De Veld et al.[20] measured the autofluorescence spectra of oral mucosa at different anatomical locations and used statistical methods like principal component analysis (PCA), artificial neural networks, and receiver operator characteristic (ROC) curves for comparison of autofluorescence and diffuse reflectance methods in distinguishing premalignant from normal/benign mucosa.[21] They observed that autofluorescence corrected for blood absorption using diffuse reflectance spectra improves the classification of cancer.

The majority of research groups[17,20,22] have used spectral features of adjoining tissues from margin areas as control in oral cancer diagnosis. These studies showed that spectroscopic changes occur not

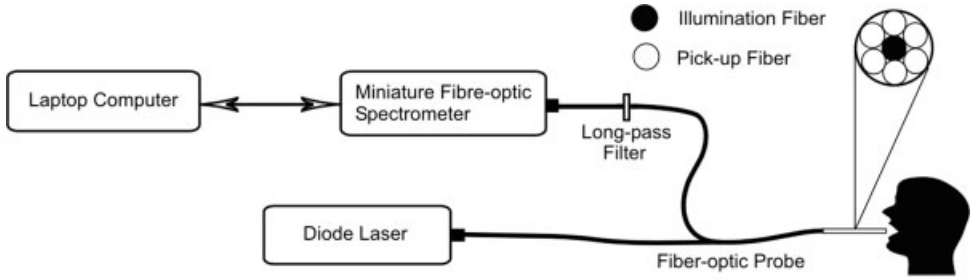

FIGURE 1. Schematic of the experimental setup for laser-induced autofluorescence spectroscopy (LIAF) measurements.

only at the center and at border of the lesion, but in the surrounding areas where no abnormalities are visible. Nevertheless, a discrimination process based on the assumption of adjoining tissues as normal or control affects the sensitivity and specificity of diagnosis.

We conducted in vivo LIAF measurements in the oral cavity of patients and healthy volunteers and generated standard reference scatterplots of fluorescence intensity ratios F500/F635, F500/705, and F500/F685 to discriminate various grades of oral cancer using site-specific database of healthy population. The spectral ratio reference standard (SRRS) thus generated was blind-tested on a subject group to check the validity of the methodology developed for diagnosis of early stages of oral cancer and the results are presented.

MATERIALS AND METHODS

Instrumentation

The laser-induced autofluorescence spectroscopy (LIAFS) system for oral cancer diagnosis, shown in Fig. 1, is comprised of a diode laser (Stocker Yale, Canada, 404 nm, 50 mW, CW) for excitation of tissue fluorophores. Light emission from the laser source is guided to the oral mucosa through a 3-m long bifurcated fiberoptic probe that has a central fiber to deliver the excitation beam and 6 surrounding fibers (400 μm diameter each) to collect LIAF emissions. The probe tip has a stainless steel ferrule, 15 cm long and 6 mm in diameter, that enabled sterilization before and after use. A black PVC sleeve of length 10 mm inserted at the probe tip maintains a fixed separation of approximately 3.5 mm between the probe tip and tissue and maximizes the fluorescence signal by providing optimum overlap between the excitation and collection areas. Because this opaque sleeve is disposable it provided extra hygiene. The light emanating from the sample was delivered to the miniature fiberoptic spectrometer (Ocean Optics, Dunedin, Fla; Model: USB 2000FL VIS-NIR), connected to the Universal Serial Bus (USB) port of a laptop computer. The long-wavelength pass filter (Schott UG420) blocks the back-scattered laser light from entering the spectrometer.

Data Acquisition

The measurement probe was kept in a plastic box containing formalin tablets for sterilization. A fiber-optic light coupler fitted on the laser head focuses and directs the laser beam onto the central fiber of the probe so that the output light projects a Gaussian intensity profile on the tissue surface. The output power at the fiber tip was maintained at 1 mW by frequent monitoring using a power/energy meter (Ophir Optronics, Israel). Slight pressure was applied on the mucosa with the sleeve tip of the probe to avoid room light from entering the detection system. The miniature fiberoptic spectrometer was fitted with a 600 lines/mm, 500 nm blazed grating for operation in the 360–1000 nm wavelength range. The detector used was a 2048-element, linear silicon CCD array and in conjunction with a 200 μm slit in the monochromator provided an optical resolution of 8 nm. The LIAF spectrum was acquired in the 420–720 nm spectral range with the help of OOI Base32 software (Ocean Optics) that was configured to record the spectra, averaged for 40 pulses, with a boxcar width of 10 nm and an integration time of 100 ms.

Study Protocol and Subjects

The study subjects included 35 healthy volunteers with no clinically observable lesions or inflammatory conditions in their oral cavity and 44 patients with clinically high-risk lesions in their oral cavity. An experienced clinician specialized in head and neck cancer identified suspicious lesions for spectral studies in each patient and recorded its visual imprint. Most of the patients had prolonged smoking or 'pan' chewing habits, whereas healthy volunteers were free from such habits and maintained good oral health and hygiene. Measurements were carried out at the outpatient clinic of the Regional Cancer Centre

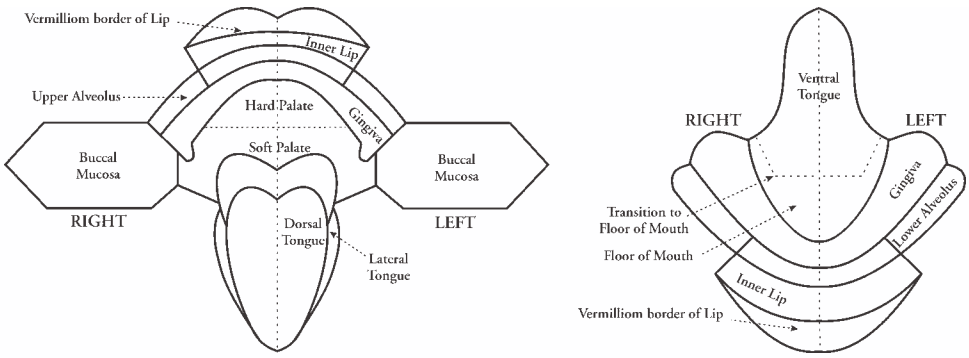

FIGURE 2. Different anatomical locations of the oral cavity for laser-induced autofluorescence spectroscopy (LIAF) measurements.

(RCC), Thiruvananthapuram, after obtaining clearance from the Ethics Committee of RCC.

Considering the heterogeneous nature of the oral cavity lesions, 15 sets of fluorescence measurements were taken from each of the suspicious lesions and adjoining healthy tissues, approximately 1 cm within the lesion boundary of the same patient, for comparison. In some subjects measurements were not possible from the adjoining mucosa, as the lesion had spread all over, whereas in others multilesions were observed.

To develop a site-specific database, fluorescence measurements were taken from 14 different anatomical sites of the oral cavity of healthy volunteers, shown in Figure 2. The LIAF spectra from 11 sites, except the vermilion border of the lip, the dorsal and the lateral sides of tongue, showed similar spectral characteristics with a broad peak at 500 nm. The mean LIAF from these 11 sites is plotted in Figure 3 along with the spectra recorded from the other 3 sites that showed dissimilar behavior. Owing to the presence of emissions at 635, 685, and 705 nm at the vermilion border of lip, the dorsal and the lateral sides of tongue, as seen in malignant lesions, these 3 sites were excluded from the study and the total sites available were limited to 61 from 37 patients. Of these 61 sites spectral ratios from 40 sites of 20 patients were used for the development of the SRRS, whereas the remaining data from 21 sites of 17 patients were used for the blind test to validate the reference standard developed.

Before initiation of measurements, the patients/volunteers were directed to hold a 0.9% saline solution in their mouth for 2 minutes to reduce the effects of recently consumed food. After completion of in vivo LIAF spectral measurements from suspicious sites and adjoining tissues, a biopsy was taken from the measurement sites and sent for histopathologic analysis after fixing in 10% formalin solution. Histology slides were prepared from the biopsies and

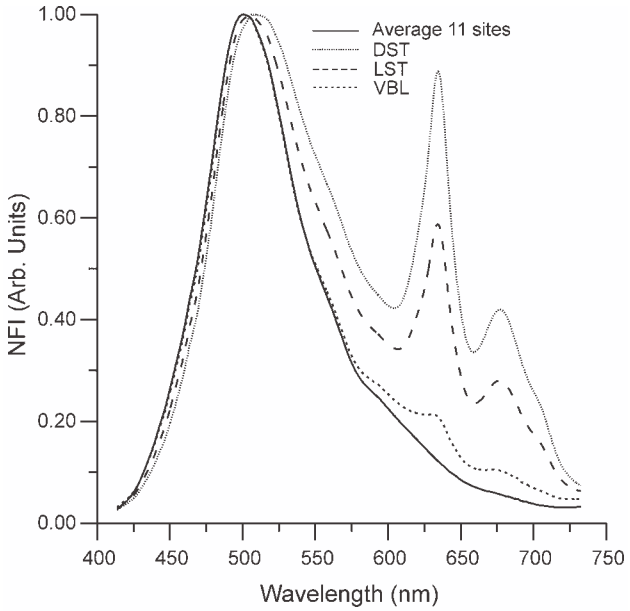

FIGURE 3. Mean laser-induced autofluorescence spectroscopy (LIAF) spectra from dorsal side of tongue (DST), lateral side of tongue (LST), and vermilion border of the lip (VBL) normalized to the autofluorescence intensity at 500 nm and compared with the average from all other 11 sites of the oral cavity. DST, LST, and VBL spectra represent the mean of 15 measurements each in 35 volunteers, whereas the average normal spectra relate to the mean of 15 measurements each at 11 sites also in 35 volunteers.

classified by an experienced pathologist who was blinded to the autofluorescence results. In the case of healthy volunteers, visual inspection was carried out instead of biopsy. After classification, spectroscopic data were correlated with the histopathologic findings. An independent Student *t*-test was performed on all 3 fluorescence intensity ratios, ie, F500/F635, F500/F685, and F500/F705 between different tissue categories, to determine the statistical significance of the fluorescence ratio method in differentiating mucosal variations.

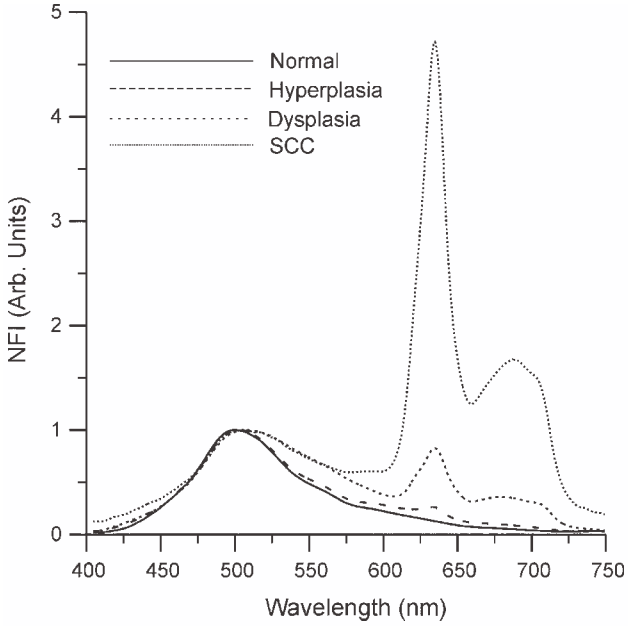

FIGURE 4. Laser-induced autofluorescence spectroscopy (LIAF) emission from different types of oral mucosa from 40 sites of 20 patients and the mean spectra from 11 sites in 35 healthy volunteers, normalized to autofluorescence emission at 500 nm. Normal spectra represent the average of $35 \times 15 \times 11$ measurements, whereas hyperplasia and dysplasia relate to 9×15 measurements and the squamous cell carcinoma (SCC) spectra is of 18×15 measurements.

RESULTS

LIAF Spectral Features

In vivo LIAF spectral measurements were taken from 40 sites of the oral cavity in 20 patients. The broad autofluorescence peak at 500 nm seen in the LIAF spectra is characteristic of all epithelial tissues. In SCC and dysplastic tissues this peak appears broadened and red-shifted by about 20 nm and 2 additional peaks due to PpIX emission are observed around 635 and 705 nm. Figure 4 shows the mean in vivo LIAF spectra of different tissue types, normalized to the intensity of the autofluorescence peak. In lesions pathologically diagnosed as SCC, the peak at 635 nm is very prominent as compared with dysplastic tissues and an additional peak around 685 nm is observed, with the 705 nm peak appearing as a shoulder. Nevertheless, the 705 nm peak is less prominent in dysplastic tissues and the 685 nm peak appears broadened. In hyperplastic tissues the 705 nm peak is absent and the intensity of the 635 peak is further reduced, whereas in healthy mucosa these 3 peaks are absent, except at the dorsal tongue, lateral tongue, and vermilion border of the lip (Fig. 3).

LIAF Intensity Ratios

Mean fluorescence intensity ratios (F500/F635, F500/F685, and F500/F705) determined from the oral mucosal spectra of 20 patients are given in Table 1, along with the results of histopathologic examination, visual, and spectral impressions. It was seen that tissues classified as normal under visual impression often had various degrees of dysplasia or hyperplasia on histopathologic examination. The spectral impression as depicted by the F500/F635, F500/F705, and F500/F685 ratios also had values that matched mostly with the histopathologic findings.

To use the ratio variations seen in Table 1 for tissue characterization, the oral mucosa was grouped into 4 categories: the first group consisted of healthy volunteer epithelium, designated as normal. The second, third, and fourth categories comprised, respectively, hyperplastic, dysplastic (premalignant), and SCC (malignant) tissues. Table 2 shows the mean F500/F635, F500/F705, and F500/F685 ratios of healthy volunteer mucosa and of patients listed in Table 1 regrouped into the above 3 distinct categories. All 3 ratios show a decreasing trend with increasing malignancy, with the lowest values for SCC and the highest for normal. The F500/F685 ratio shows a maximum variation of 45% between normal and hyperplastic tissues and 68% between hyperplastic and dysplastic tissues, whereas between dysplastic and SCC tissues the F500/F705 ratio shows a variation of 75%.

SRRS for Tissue Characterization

Figure 5a-c shows the scatterplots of the spectral intensity ratios F500/F635, F500/F705, and F500/F685 from 40 sites in 20 patients, categorized as hyperplasia, dysplasia, and SCC, along with the site-specific mean normal data from 35 healthy volunteers. Discrimination lines were drawn between the normal and hyperplastic, hyperplastic and dysplastic, dysplastic and SCC at values that correspond to the average ratio values of the respective groups. For example, in the case of healthy volunteers the average F500/F635, F500/F685, and F500/F705 ratio values were 8.00, 33.68, and 27.61, respectively. The cutoff lines for discriminating the normal from hyperplastic were drawn at values corresponding to the mean of the healthy volunteer ratios and those of hyperplastic mucosa (6.16, 21.57, and 15.1, respectively) in patients. The classification sensitivity and specificity in discriminating each of these categories were determined based on the discrimination threshold values, by validation with the gold standard, ie, histopathologic results of biopsy from LIAF measurement sites.

TABLE 1
Fluorescence Intensity Ratio F500/F635, F500/F705, and F500/F685 of Patients Included in the SRRS and Their Histopathologic, Visual, and Spectral Impressions

Patient no.	Site	HI	VI	F500/F635	SI	F500/F705	SI	F500/F685	SI
1	Buccal	Dysplasia	Homogeneous leukoplakia	2.20	Dysplasia	6.10	Dysplasia	5.10	SCC
	Buccal	Hyperplasia	Normal	5.23	Hyperplasia	16.46	Hyperplasia	11.68	Hyperplasia
2	Buccal	Dysplasia	Erythroplakia	2.17	Dysplasia	4.47	SCC	3.48	Dysplasia
	Buccal	Dysplasia	Normal	3.85	Dysplasia	9.05	Dysplasia	5.96	Dysplasia
3	Buccal	HSSCC	Proliferative growth	0.34	SCC	1.05	SCC	0.75	SCC
	Buccal	Dysplasia	Normal	3.48	Dysplasia	6.88	Dysplasia	4.72	Dysplasia
4	Buccal	Dysplasia	Growth	1.49	SCC	2.82	SCC	2.28	SCC
5	Alveolus	SCC	Ulcerative lesion	0.97	SCC	2.02	SCC	1.71	SCC
	Alveolus	Hyperplasia	Normal	5.85	Hyperplasia	20.00	Hyperplasia	14.21	Hyperplasia
6	Floor of mouth	SCC	Proliferative growth	0.76	SCC	1.88	SCC	1.49	SCC
	Floor of mouth	Hyperplasia	Normal	5.33	Hyperplasia	16.68	Hyperplasia	11.95	Hyperplasia
7	Alveolus	SCC	Proliferative lesion	0.65	SCC	1.68	SCC	1.33	SCC
	Alveolus	Dysplasia	Normal	2.52	Dysplasia	6.94	Dysplasia	5.24	Dysplasia
8	Buccal	SCC	Growth	0.16	SCC	0.54	SCC	0.41	SCC
9	Buccal	SCC	Verricous lesion	1.45	SCC	3.77	SCC	2.88	SCC
	Buccal	Hyperplasia	Normal	6.30	Hyperplasia	24.56	Normal	16.49	Hyperplasia
10	Alveolus	HSSCC	Ulcerative proliferate lesion	1.39	SCC	2.11	SCC	1.87	SCC
	Alveolus	Hyperplasia	Normal	8.05	Normal	36.94	Normal	24.62	Normal
11	Buccal	Dysplasia	Verricous Leukoplakia	3.25	Dysplasia	12.45	Dysplasia	5..55	Dysplasia
	Buccal	Normal	Normal	7.04	Hyperplasia	34.17	Normal	21.46	Hyperplasia
12	Buccal	SCC	Leukoplakia	3.10	Dysplasia	5.91	Dysplasia	5.01	Dysplasia
	Buccal	Hyperplasia	Normal	6.99	Hyperplasia	18.01	Hyperplasia	13.95	Hyperplasia
13	Buccal	Dysplasia	Leukoplakia	3.23	Dysplasia	11.30	Dysplasia	6.26	Dysplasia
	Buccal	Hyperplasia	Normal	5.86	Hyperplasia	25.31	Normal	16.11	Hyperplasia
14	Alveolus	SCC	Ulcerative proliferate lesion	1.03	SCC	2.95	SCC	2.37	SCC
	Alveolus	Normal	Normal	7.33	Normal	33.30	Normal	20.68	Hyperplasia
15	Buccal	SCC	Verricous lesion	0.38	SCC	1.45	SCC	1.10	SCC
	Buccal	Normal	Normal	9.02	Normal	43.92	Normal	26.53	Normal
16	Buccal	SCC	Ulcerative proliferate growth	1.32	SCC	4.01	SCC	3.36	Dysplasia
	Buccal	Normal	Normal	6.92	Hyperplasia	24.20	Hyperplasia	16.84	Hyperplasia
17	Buccal	SCC	Proliferate growth	1.32	SCC	2.83	SCC	2.25	SCC
	Buccal	Hyperplasia	Normal	4.93	Hyperplasia	12.03	Hyperplasia	10.10	Dysplasia
18	Buccal	SCC	Ulcerative proliferate growth	0.13	SCC	0.45	SCC	0.41	SCC
	Buccal	Hyperplasia	Normal	6.99	Hyperplasia	18.9	Hyperplasia	13.95	Hyperplasia
19	Lower Alveolus	SCC	Ulcerative proliferate growth	0.26	SCC	0.92	SCC	0.58	SCC
	Lower Alveolus	Dysplasia	Normal	2.26	Dysplasia	5.84	Dysplasia	3.76	Dysplasia
20	Floor of mouth	SCC	Proliferate growth	0.24	SCC	0.79	SCC	0.71	SCC
	Buccal	SCC	Leukoplakia	0.45	SCC	1.56	SCC	1.24	SCC
	Buccal	SCC	Proliferate growth	0.27	SCC	0.88	SCC	0.78	SCC
	Inner lip	SCC	Proliferate growth	0.17	SCC	0.56	SCC	0.49	SCC

HI indicates histopathologic impression; SCC, squamous cell carcinoma; VI, visual impression; HSSCC, highly suspicious SCC; SI, spectral impression.

TABLE 2
Mean Autofluorescence Spectral Ratios in a Healthy Population and Patients Categorized According to Different Grades

Histologic diagnosis	Population no.	F500/F635 no. (%)	F500/F705 no. (%)	F500/F685 no. (%)
Normal, healthy	35	8.00 ± 0.66	33.08 ± 5.71	27.61 ± 3.74
Hyperplasia	9	6.16 ± 1.00 (23)	21.57 ± 7.26 (35)	15.10 ± 4.26 (45)
Dysplasia	9	2.78 ± 0.80 (55)	7.61 ± 3.17 (65)	4.82 ± 1.33 (68)
Squamous cell carcinoma	18	0.80 ± 0.74 (71)	1.96 ± 1.46 (75)	1.6 ± 1.2 (67)

The percentage given in parentheses denotes the change with respect to the next lower grade.

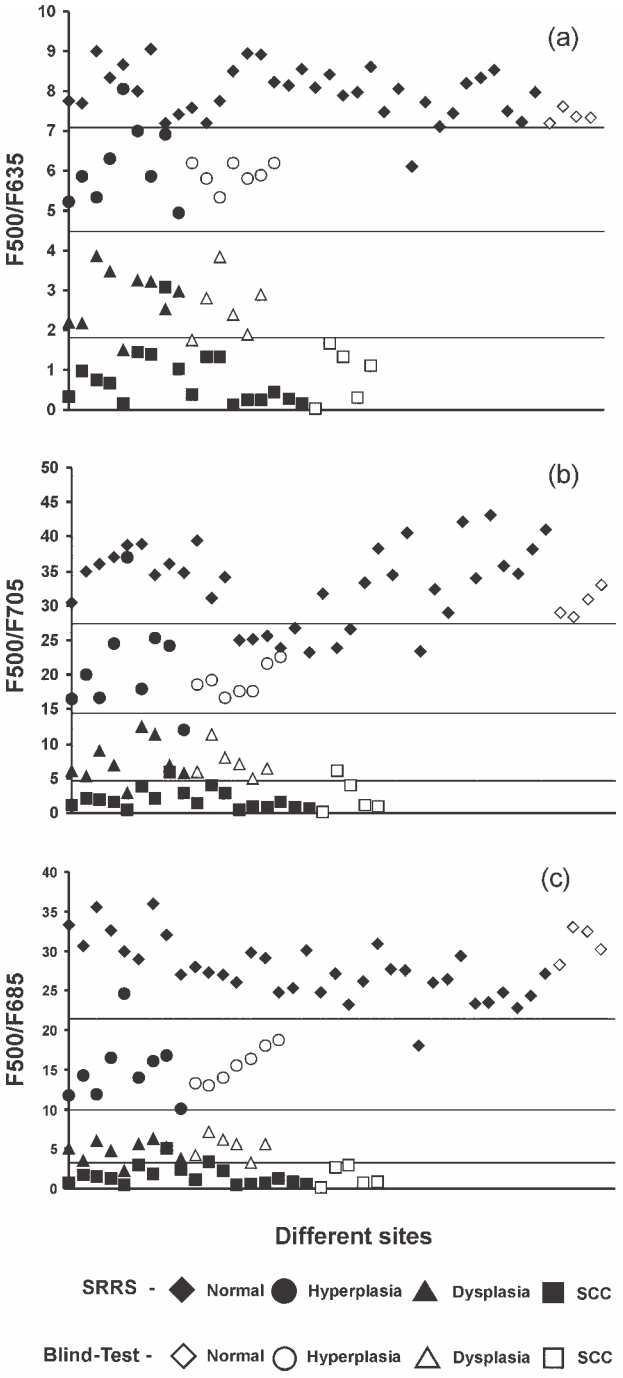

FIGURE 5. Spectral ratio reference standard (SRRS) developed from 35 healthy subjects and 40 sites in 20 patients for fluorescence intensity ratios (a) F500/F635, (b) F500/F705, and (c) F500/F685. The solid symbols represent SRRS, whereas the open symbols relate to the blind test results at 21 sites in 17 patients.

DISCUSSION

LIAF Spectral Features

Many research groups have reported the autofluorescence around 500 nm as an emission from endogenous fluorophores, like NADH, FAD, collagen, elastin, and amino acids, and emissions at 635 and 705 nm from enhanced PpIX presence in malignant tissues.[4–6,10–12,23,24] In addition to these peaks, we noticed a prominent peak around 685 nm in malignant tissues that appears between the PpIX peaks. In dysplastic tissues this peak is not very prominent, as in SCC, but its presence contributes effectively to broaden the 705 nm peak. High-performance liquid chromatograms of tumor and normal colorectal tissues have shown the presence of a higher concentration of corproporphyrinIII in malignant tissues.[23] In the same study, peaks at 630 and 685 nm were observed when corproporphyrinIII dissolved in methanol was excited with 505 nm light. We can thus conclude that the peak observed at 685 nm, especially in SCC and dysplastic tissues, could be attributed to the accumulation of endogenous fluorophore corproporphyrinIII, which is a precursor of PpIX in the heme synthesis, and not because of chlorophyll fluorescence from leafy food items,[20] as this peak was absent in healthy volunteer tissues.

Sensitivity and Specificity With SRRS

Most of the patients who participated in our study had smoking, chewing, or alcohol consumption habits that could alter the adjoining and contralateral tissue structure. In many, the lesion spread was often large and it was not possible to identify a suitable adjoining or contralateral mucosa for control measurements. As compared with the mean spectral ratios of a healthy population given in Table 2, the adjoining mucosa of Patients 11, 14, 15, and 16, shown in Table 1 and identified visually and pathologically as normal, had lower ratios, signifying hyperplasia. Slaughter et al.[25] reported that the long-term influence of carcinogens like tobacco, smoke, and alcohol on the oral mucosa leads to "field cancerization" and influences diagnosis. Hence, measurements from these 4 sites were excluded in the development of our reference database. Furthermore, we overcame the dependence on the adjoining mucosa as control by use of a site-specific healthy population database (Table 2).

De Veld et al.[20] in a study on 97 healthy volunteers observed the 635 nm porphyrin emission only from the dorsal side of the tongue and vermilion border of the lip. In our studies, the lateral tongue also showed an emission peak at 635 nm (Fig. 3).

TABLE 3
Sensitivity and Specificity of SRRS in Discriminating Different Tissue Types in 20 Patients and Results of Blind-Test Validation in 17 Patients

		Normal vs hyperplasia		Hyperplasia vs dysplasia		Dysplasia vs squamous cell carcinoma	
	LIAF ratios	Sensitivity	Specificity	Sensitivity	Specificity	Sensitivity	Specificity
SRRS results	F500/F635	89	97	100	100	95	86
	F500/F685	89	97	100	100	95	86
	F500/F705	89	74	100	89	95	86
	Over all	89	89	100	96	95	86
Blind-test results	F500/F635	100	100	100	100	100	83
	F500/F685	100	100	100	100	100	100
	F500/F705	100	100	100	100	80	100
	Overall	100	100	100	100	93	94

LIAF indicates laser-induced autofluorescence spectroscopy; SRRS, spectral ratio reference standard.
Independent Student *t*-test, $P < .001$ for each discrimination group.
Sensitivity indicates abnormal spectroscopy and/or abnormal histopathology; specificity indicates normal spectroscopy and/or normal histopathology.

Furthermore, we observed peaks at 685 and 705 nm, in particular at the dorsal and lateral side of the tongue, whereas in the vermilion border of lip these peaks were less intense. Because the ratio values from these 3 anatomical locations were excluded in the SRRS developed, it could be suitable for discrimination of oral cancer at all the anatomical locations except the vermilion border of the lip, dorsal tongue, and lateral border of tongue, for which a separate spectral reference database would be required.

Sensitivity and specificity of discrimination using SRRS were determined from the cutoff values given in Figure 5a-c. For the F500/F635 ratio, by selecting a cutoff at the mean (7.08) of normal and hyperplastic values, a sensitivity and specificity of 89% and 97%, respectively, was obtained to discriminate normal from hyperplastic mucosa. In the same plot the cutoff drawn at 1.79 discriminates premalignant dysplastic tissues from malignant SCC with a sensitivity and specificity of 95% and 86%, respectively. Furthermore, an overall sensitivity and specificity of 89% was achieved for distinguishing normal from hyperplasia, whereas a sensitivity and specificity of 100% and 96%, respectively, was obtained to distinguish dysplasia from hyperplasia. Table 3 illustrates independent and overall sensitivities and specificities of F500/F635, F500/F685, and F500/F705 SRRS for differentiating the 4 different mucosal variations. All 3 ratios used to differentiate the tissue categories have very low independent Student *t*-test values, $P < .001$.

We confined fluorescence measurements to a circular area of 6 mm in diameter at the selected site and the average of 15 measurements represents the spectra of each site. However, the biopsy samples (approximately 2 mm in diameter) for histopathology were taken only from a portion within the measurement area. The finding that an oral lesion can be malignant at 1 site, whereas it can be premalignant a few millimeters away, could be the reason for the lower sensitivities and specificities reported in Table 3 for standard reference database.

Spectral impressions given in Table 1 depend on the location of the spectral ratios in the SRRS plots. Although the lesions from the margin areas were seen clinically as normal, the spectral impressions based on reference scatterplots have identified these sites as dysplastic or hyperplastic, and our spectral diagnosis matches well with histopathologic findings in most cases. Furthermore, using these standard plots we could accurately categorize the lesions that appeared as ulcerative proliferate growth for the clinicians, but identified histopathologically as SCC. Clinical examinations are often capable of identifying lesions as normal or abnormal, and pathologic examination of biopsy is the accepted practice for classifying them as hyperplasia, dysplasia, or SCC.

Clinically, leukoplakias are treated as low/high-risk lesions, which are generally diagnosed pathologically as hyperplasias, with or without mild to moderate dysplasia. The reference scatterplots discriminated SCC sites that were misclassified clinically as leukoplakias in the case of Patient 20 (Table 1). The study shows that the spectral impressions methodology developed could act as an adjunct to clinicians in tissue differentiation and facilitate speedy diagnosis at the clinic to arrive at appropriate follow-up treatment or surgery. Furthermore, in some cases even pathologic examination was not able to classify the samples correctly as SCC (Patients

TABLE 4
Spectral Ratios From 17 Patients Used in SRRS Validation With Their Histologic and Clinical Impressions

Patient no.	Site	Histopathology	Visual impression	F500/F635	F500/F705	F500/F685
1	Alveolus	Dysplasia	Ulcerative proliferative growth	1.74	5.90	4.19
	Alveolus	Hyperplasia	Normal	6.2	18.62	13.3
2	Buccal mucosa	Dysplasia	Leukoplakia	2.80	11.43	7.12
3	Buccal mucosa	SCC	Verricous lesion	0.04	0.14	0.12
4	Inner lip	SCC	Verricous lesion	1.70	6.12	2.64
	Inner lip	Dysplasia	Normal	3.83	8.05	6.18
5	Buccal mucosa	SCC	Ulcerative proliferative growth	1.32	4.01	3.00
	Buccal mucosa	Hyperplasia	Normal	5.81	19.29	13.07
6	Floor of mouth	Dysplasia	Verricous growth	2.4	7	5.64
7	Hard palate	SCC	Proliferative growth	0.29	1.06	0.65
8	Buccal mucosa	Dysplasia	Leukoplakia	1.90	4.97	3.22
9	Ventral tongue	SCC	Ulcerative proliferate lesion	1.12	1.02	0.82
	Ventral tongue	Dysplasia	Normal	2.9	6.34	5.56
10	Buccal mucosa	Hyperplasia	Normal	5.34	16.65	14
	Buccal mucosa	Hyperplasia	Normal	6.2	17.6	15.5
11	Buccal mucosa	Hyperplasia	Homogeneous leukoplakia	5.8	17.62	16.3
12	Inner lip	Hyperplasia	Homogeneous leukoplakia	5.9	21.6	18
13	Gingiva	Hyperplasia	Ulcer	6.2	22.6	18.7
14	Buccal mucosa	Normal	Normal	7.2	29.2	28.2
15	Buccal mucosa	Normal	Normal	7.6	28.33	33
16	Buccal mucosa	Normal	Normal	7.35	31	32.45
17	Buccal mucosa	Normal	Normal	7.32	33	30.23

SRRS indicates spectral ratio reference standard; SCC, squamous cell carcinoma.

3 and 10 in Table 1). These cases were classified correctly as highly suspicious SCC (HSSCC), but generally confirmed as SCC, after taking into consideration the opinion of the clinician.

SRRS Validation

To test the reliability of the developed SRRS, a blind-test was carried out in a new group of 17 patients. Table 4 shows the site location, histopathologic and visual impressions, and the 3 spectral ratios. For validation, the 3 spectral ratios from 21 sites of these patients were inserted in the SRRS developed (Fig. 5a-c) and the results were correlated with histopathologic findings. The sensitivity and specificity values for discriminating different tissue transformations during the blind test are given in Table 3. It is seen that SRRS discriminates normal mucosa from hyperplastic, and hyperplastic from dysplastic mucosa, with 100% sensitivity and specificity. An overall sensitivity of 93% and specificity of 94% was achieved in discriminating 5 SCC lesions from 6 dysplastic tissues. In addition, the ulcerated lesion observed clinically as hyperplasia in Patient 10 was found to be in agreement with the gold standard (Table 4).

Zheng et al.[17] used scatterplots of the red-blue intensity ratio to differentiate benign tissues (consisting of hyperplasia and inflammation) from malignant oral tissues (that include dysplasia, SCC, and CIS) with a sensitivity and specificity of 92% and 93%, respectively. In contrast, the SRRS scatterplots simultaneously differentiated mucosal variations such as hyperplasia, dysplasia, and SCC from normal with better sensitivities and specificities, as given in Table 3. It may be noted that all 3 ratios gave 100% sensitivity and specificity for early discrimination of tissue transformation from hyperplasia to dysplasia. As regards discrimination of dysplasia from SCC, the F500/F685 ratio gives 100% sensitivity and specificity, whereas the commonly used F500/F635 ratio has a sensitivity of 100% and specificity of 83%. The sensitivity and specificity given in Table 3 for blind tests are also higher than earlier reports[14,17,22] and were obtained without the use of ALA or any other exogenous photosensitizer.

Conclusions

The noninvasive in vivo LIAF diagnostic modality described in this article provides a reliable means to understand tissue progression toward malignancy, without the use of an exogenous photosensitizer. The SRRS scatterplots developed give improved sensitivity and specificity as compared with earlier reports and matches well with the gold standard. Therefore, the methodology developed could act as an adjunct to clinicians for early discrimination of oral dysplasias

and hyperplasias. Among the 3 ratios studied, the F500/F685 ratio was more suited to understand tissue progression from normal to premalignant and malignant with 100% sensitivity and specificity. Our results confirm that the distinction between the normal and diseased tissues within a patient is difficult and could lead to false classification or low specificities, as in most of the cases; tissues surrounding the lesion show various degrees of dysplasia. Currently, we are working toward extending clinical trials to other sites of the oral cavity that were excluded in this study and to explore possibilities for detection of high-risk lesions like erythroplakia and submucosal fibrosis and to use the SRRS as a tool for precise delineation of lesion margin during surgical interventions.

REFERENCES

1. Wingo PA, Tong T, Bolden S. Cancer statistics. *CA Cancer J Clin*. 1995;45:8–30.
2. Boone C, Bacus JW, Bacus JV, et al. Properties of intraepithelial neoplasia relevant to cancer chemopreventation and the development of surrogate for clinical trials. *Proc Soc Exp Biol Med*. 1997;216:151–165.
3. Evan GI, Vousden KH. Proliferation, cell cycle and apoptosis in cancer. *Nature (Lond)*. 2001;411:342–348.
4. Wagnieres GA, Star WM, Wilson BC. In vivo fluorescence spectroscopy and imaging for oncological applications. *Photochem Photobiol*. 1998;68:603–632.
5. Schomacker KT, Fusoli JK, Compton CC, et al. Ultraviolet laser induced fluorescence of colonic tissue: basic biology and diagnosis potential. *Lasers Surg Med*. 1992;12:63–78.
6. Ramanujam N, Mitchell MF, Mahadevan A, et al. In vivo diagnosis of cervical intraepithelial neoplasia using 337-nm-excited laser induced fluorescence. *Proc Natl Acd Sci U S A*. 1994;91:10193–10197.
7. Qu JY, Wing P, Huang Z, et al. Preliminary study of in vivo autofluorescence of nasopharyngeal carcinoma and normal tissue. *Lasers Surg Med*. 2000;26:432–440.
8. Schantz SP, Kolli V, Savage HE, et al. In vivo native cellular fluorescence and histological characteristics of head and neck cancer. *Clin Cancer Res*. 1998;4:1177–1182.
9. Eker C, Rydell R, Svanberg K, et al. Multivariate analysis of laryngeal fluorescence spectra recorded in vivo. *Lasers Surg Med*. 2001;28:259–266.
10. Richards-Kortum R, Sevick-Muraca E. Quantative optical spectroscopy for tissue diagnosis. *Annu Rev Phys Chem*. 1996;47:555–606.
11. Drezek R, Sokolov K, Utzinger U, et al. Understanding the contributions of NADH and collagen to cervical tissue fluorescence spectra. Modeling, measurements, and implications. *J Biomed Opt*. 2001;6:385–396.
12. Ingrams DR, Dhingra JK, Roy K, et al. Autofluorescence characteristics of oral mucosa. *Head Neck*. 1997;19:27–32.
13. Heintzelman DL, Utzinger U, Fuchs H, et al. Optimal excitation wavelengths for in vivo detection of oral neoplasia using fluorescence spectroscopy. *Photochem Photobiol*. 2000;72:103–113.
14. Gillenwater A, Rhonda J, Ravi G, et al. Noninvasive diagnosis of oral neoplasia based on fluorescence spectroscopy and native autofluorescence. *Arch Otolaryngol Head Neck*. 1998;124:1251–1258.
15. Savage H, Kolli V, Ansley J, Chandawarkar R, Alfano R, Schantz S. Innate tissue fluorescence of the oral mucosa of controls and head and neck cancer patients. In: Alfano RR, ed. Proceedings of Advances in Lasers and Light Spectroscopy to Diagnose Cancer and Other Diseases II. Bellingham, Wash: SPIE; 1995:2387:2–14.
16. Scott MA, Hopper C, Sahota A, et al. Fluorescence photodiagnostics and photobleaching studies of cancerous lesions using ratio imaging and spectroscopic techniques. *Lasers Med Sci*. 2000;15:63–72.
17. Zheng W, Khee CS, Ranjiv S, et al. Detection of neoplasms in the oral cavity by digitized endoscopic imaging of 5-aminolevulinic acid-induced protoporphyrin IX fluorescence. *Int J Oral Onc*. 2002;21:763–768.
18. Svistun E, Alizadeh-Naderi R, El-Naggar A, Jacob R, Gillenwater A, Richards-Kortum R. Vision enhancement system for detection of oral cavity neoplasia based on autofluorescence. *Head Neck*. 2004;26:205–215.
19. Lane PM, Gilhuly T, Whitehead P, et al. Simple device for the direct visualization of oral-cavity tissue fluorescence. *J Biomed Opt*. 2006;11:024006.
20. De Veld DC, Marina S, Max JHW, et al. Autofluorescence characteristics of healthy oral mucosa at different anatomical sites. *Lasers Surg Med*. 2003;23:367–376.
21. De Veld DC, Marina S, Max JHW, Robert PWD, Sterenborg HJCM, Jan LNR. Autofluorescence and diffuse reflectance spectroscopy for oral oncology. *Lasers Surg Med*. 2005;36:356–364.
22. Af Klitenberg C, Wang I, Charlotta L, et al. Laser-induced fluorescence studies of premalignant and benign lesions in female genital tract. In: Bigio IJ, Svanberg K, Sehncekenberger H, Salik J, Viallet PM, eds. Optical Biopsies and Microscopic Techniques II.Proc SPIE 1997;3197:34–40.
23. Moesta KT, Bernd E, Tim H, et al. Protoporphyrin IX occurs naturally in colorectal cancers and their metastases. *Cancer Res*. 2001;61:991–999.
24. DaCosta RS, Anderson H, Wilson B. Molecular fluorescence excitation-emission matrices relevant to tissue spectroscopy. *Photochem Photobiol*. 2003;78:384–392.
25. Slaughter D, Southwick H, Smejkal W. Field cancerization in oral stratified squamous epithelium. *Cancer*. 1953;6:963–968.